IEEE Access
Multidisciplinary | Rapid Review | Open Access Journal

Received August 6, 2020, accepted August 15, 2020, date of publication August 18, 2020, date of current version August 27, 2020.

Digital Object Identifier 10.1109/ACCESS.2020.3017693

A Novel Conductivity Classification Technique for Non-Magnetic Tilting Metals by Eddy Current Sensors

YUE DU[1], ZHIJIE ZHANG[1], (Member, IEEE), WULIANG YIN[1,2], (Senior Member, IEEE), SHUANG ZHU[2], HANYANG XU[2], AND ZIQI CHEN[2]

[1]School of Instrument and Electronics, North University of China, Taiyuan 030051, China
[2]School of Electrical and Electronic Engineering, The University of Manchester, Manchester M13 9PL, U.K.

Corresponding authors: Zhijie Zhang (zhangzhijie@nuc.edu.cn) and Wuliang Yin (wuliang.yin@manchester.ac.uk)

This work was supported in part by the Shanxi International Science and Technology Cooperation Project under Grant 201803D421038, and in part by the Shanxi 1331 Project Key Subject Construction.

ABSTRACT The classification of conductivity is significant for recycling metallic scraps. The eddy current sensor is distinct from other classification methods by its merits of non-contact, economical set-up, fast measuring, and so forth. By introducing a set-up that could ensure the single-valued mutual inductance trajectory on the complex plane, we propose the circle fitting method to extract the global features of different trajectories. It is subsequently observed that the fitting circle centers-one of the global features-for the same conductivity with various tilting angles are distributed longitudinally close to each other. The feature line, which is parallel to the abscissa axis, is introduced to represent this gathering distribution behavior. The feature lines for different conductivity are distinguishable. Thus, we construct a simple classification method with only two steps. The test results show great fidelity of the proposed classification technique which can successfully classify the tilting metallic samples within 11.3°.

INDEX TERMS Non-magnetic metal, tilting, conductivity classification, eddy current sensors, circle fitting.

I. INTRODUCTION

The reuse of metallic scraps becomes more important recently because of the shortage of resources on earth. One of the most attractive ways to address this problem is metal classification. There are several methods that currently prevail in classifying metallic fragments. The first one is the heavy media separation [1] which could separate metallic scraps of which densities need to be significantly different. The second one is image recognition which distinguishes metals based on analyzing the color information [2], [3]. There are also other methods such as the laser-induced breakdown spectroscopy [4], [5], X-ray beam absorption [6], and so forth. Even though these methods have undoubted advantages, the drawbacks are non-negligible. The method of heavy media separation is unable to classify metals with comparable densities [7]. The image recognition may lose fidelity if the metal surfaces have colored coating. The methods of laser-induced breakdown spectroscopy and X-ray beam absorption are almost the most reliable, which, however, resort to expensive devices and demanding surroundings.

The eddy current sensor is also capable of classifying metals [8]. It starts with exciting time-variant electromagnetic fields which then form eddy current inside metals. This eddy current is varying with the conductivity, which subsequently produces the secondary magnetic field [9]. After picked up by the receiving coil, the secondary magnetic field induces electric current which would finally be measured by the impedance analyzer. The eddy current sensor is widely used in non-destructive test [10]–[12] due to non-contact, fast measuring, and economical devices. In [13]–[15], eddy current sensors are utilized to measure the conductivity. One of the intriguing conclusions is that the square of the phase of the impedance is proportional to the conductivity when the thickness of the sample is more than four times the skin depth [15]. This conclusion is also drawn in the form of logarithm [16]. In other words, the logarithm of the phase of the impedance is proportional to the logarithm of the conductivity. However, this conclusion is not applicable to samples with tilting surfaces which prevail in metallic scraps. Recently,

The associate editor coordinating the review of this manuscript and approving it for publication was Kan Liu.

the combination of eddy current sensors and photoelectric sensors is used to classify metals with tilting surfaces [8] by detecting the tilting angle through photoelectric sensors and then resorting to the characteristic phases. Although the conductivity classification of tilting samples within 9.0° is achieved, double usages of the method of linear fitting on the data obtained by photoelectric sensors and eddy current sensors would introduce more error into the classification results.

In this article, we manage to classify metallic samples with tilting surfaces using only eddy current sensors and the classifiable tilting angle is extended to 11.3° larger than 9.0° reported before [8]. In Section II we give a detailed introduction to our set-up by only using eddy current sensors. The measurement through this set-up is dynamic in which the lift-off is changing with time. In Section III we describe the circle fitting method to extract global features from the mutual inductance trajectories. Based on the circle fitting method, in Section IV it is shown that the fitting circle centers are distributed close to a feature line (parallel to the abscissa axis) for the same conductivity with various tilting angles. The classification technique is subsequently proposed by finding the minimum distance between the input fitting circle center and different feature lines. Finally, some tests are conducted to show the fidelity of this classification technique, by which tilting metallic samples within 11.3° are successfully classified.

II. EXPERIMENTAL SET-UP

The model built in [8] has tilting samples moving across the eddy current sensor, which, although easily to be operated, introduces asymmetry into the mutual inductance trajectory. This may be the reason why the trajectory in the complex plane is multi-valued (in other words, the mutual inductance trajectory is not a curve but a loop), which makes it hard to find a global feature to characterize the whole trajectory. As is shown in Fig. 1, we propose another set-up where the measured mutual inductance trajectory is single-valued from which it is easier to extract global features. In this set-up, the rotation axis of the sample is the x-axis and the moving direction of the probe is along the z-axis. The main difference between this experimental set-up and others [17], [18] is that the lift-off is not an unwanted effect but an independent variable. In this work, the thickness of the sample is 1cm which is much larger than the skin depth under the 40KHz excitation signal. The entire classification system is shown in Fig. 2 where there are an EM instrument [19] for signal processing, a transformer for calibration [20], a host computer, a scanning stage, a probe wrapping eddy current sensors inside and several samples. The analytical expression for this model with a non-tilting sample firstly given by Dodd and Deed is theoretically only applicable to the sample which has an infinitely large surface [21], but the improved analytical expression for the sample with the finite size is recently derived in [22]. The integral range in this improved analytical expression is $(3.518/r, \infty)$ where r is the radius

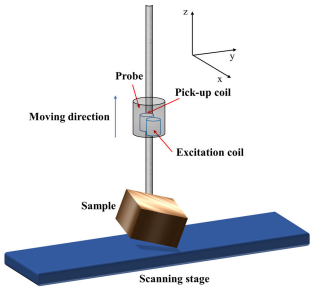

FIGURE 1. Diagram of the whole classification system consisting of the scanning stage, a sample and a probe.

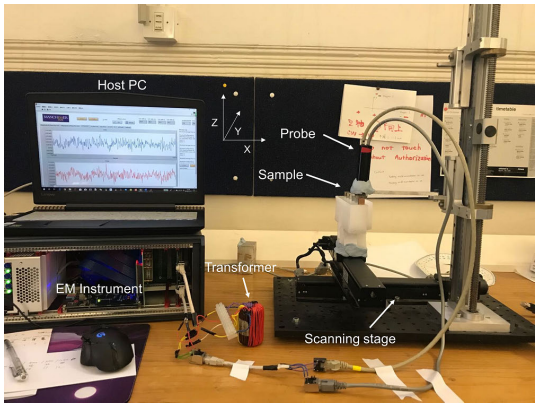

FIGURE 2. Experimental set-up [8] consisting of an EM instrument for signal processing, a transformer for calibration, a host computer, a scanning stage, a probe wrapping eddy current sensors inside and several samples.

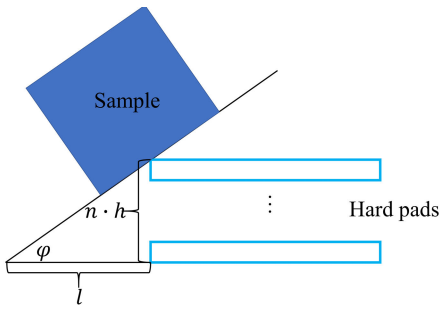

FIGURE 3. Diagram of how to tilt the metallic sample in the experiments.

of the sample, which is different from the range $(-\infty, \infty)$ in Dodd's analytical expression. However, the model with a tilting sample still has not been analyzed to the best of our knowledge. The diagram of how to tilt the metallic sample in our experiment is shown in Fig. 3. The tilting angle φ is given by

$$tan\varphi = \frac{nh}{l} \tag{1}$$

where n is the number of hard pads, h is 0.5mm (the height of one pad) and l is 1cm in the experiment. The measured mutual inductance trajectories for different conductivity with various tilting angles are shown in Fig. 4 where the trajectory

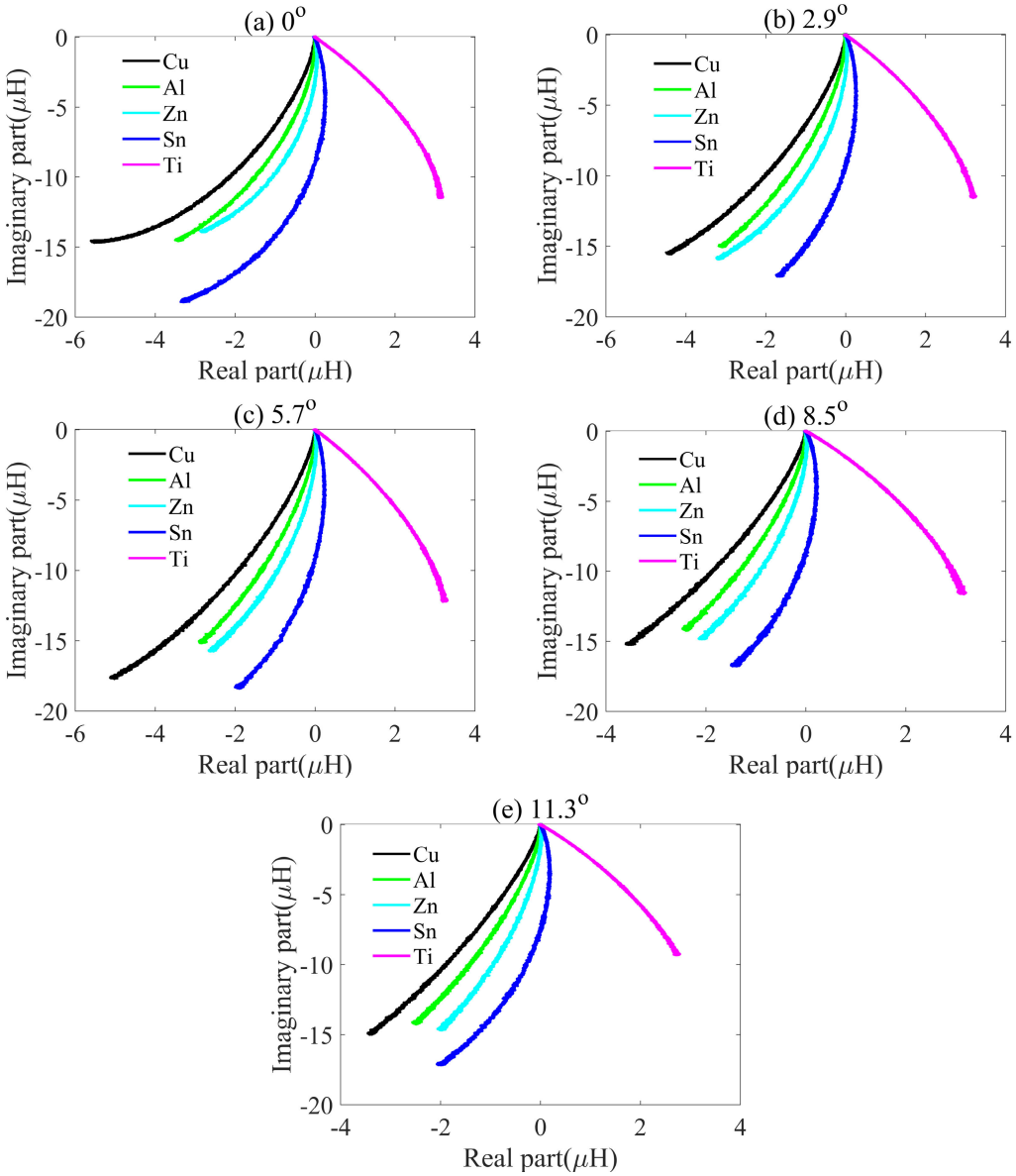

FIGURE 4. Mutual inductance trajectories of five metallic samples measured by moving the probe along z-axis when the tilting angle is (a) 0°. (b) 2.9°. (c) 5.7°. (d) 8.5°. (e) 11.3°. The trajectories are single-valued and rotating counter-clockwise when the conductivity becomes smaller.

is rotating counter-clockwise when the conductivity becomes smaller. In other words, in Fig. 4 the real part of mutual inductance becomes larger from copper to titanium with the same imaginary part. The measured mutual inductance is given by

$$L = L_R + iL_I \tag{2}$$

$$\Delta L = L - L_{air} \tag{3}$$

where L_{air} is the measured mutual inductance when no sample exists.

$$\Delta L = |\Delta L| e^{i\theta} \tag{4}$$

TABLE 1. Conductivity of metal.

Metal	Conductivity (S/m)
Copper	5.96×10^7
Aluminum	3.77×10^7
Zinc	1.69×10^7
Tin	0.92×10^7
Titanium	0.24×10^7

where θ is the phase. The reason why the phase changes along the trajectory maybe the finite size of the sample, which is different from the phase spectral, almost free from the lift-off, for the sample of an infinite size [23].

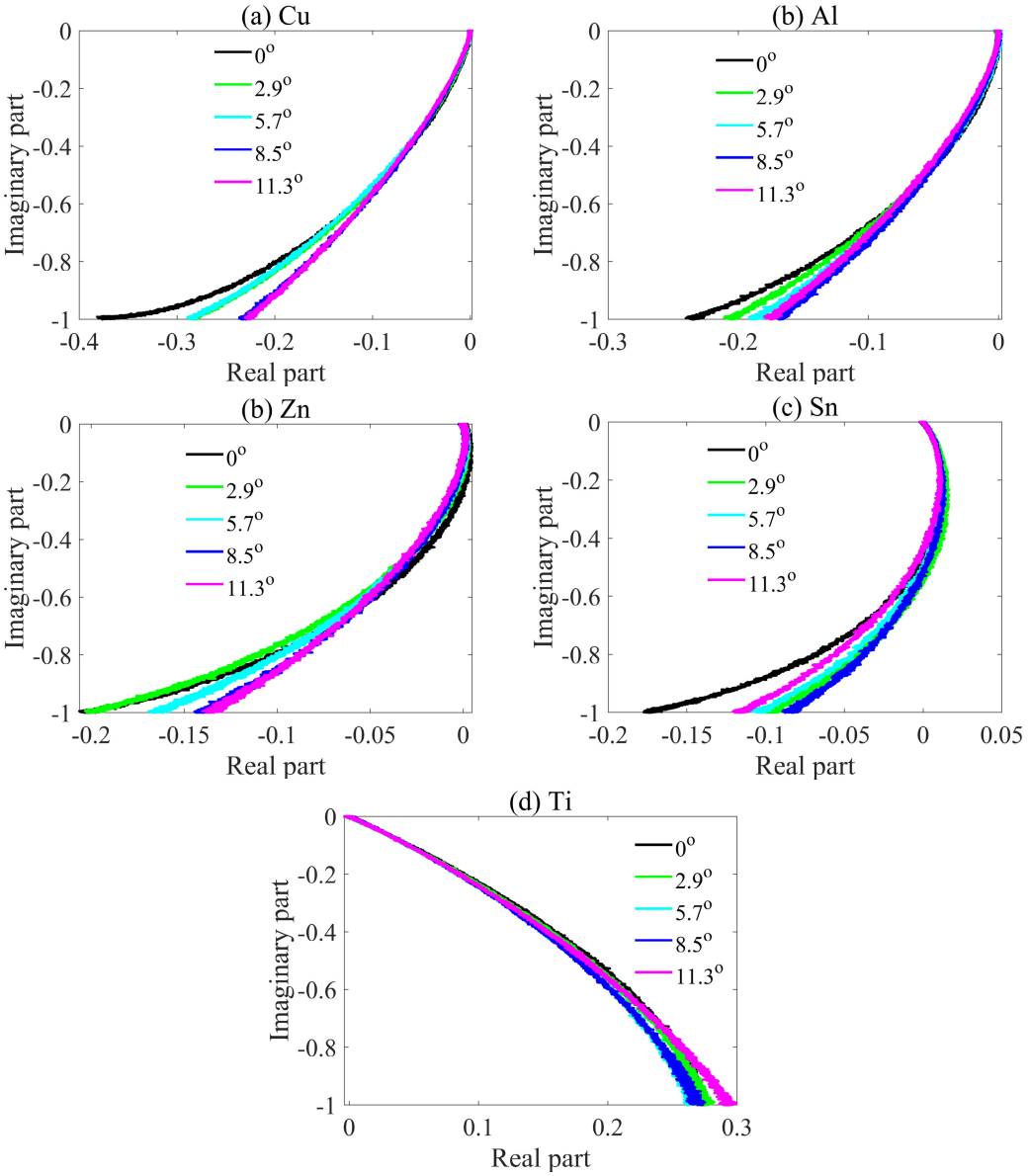

FIGURE 5. Mutual inductance trajectories of (a) Copper. (b) Aluminum. (c) Zinc. (d) Tin. (e) Titanium after normalized to the maximum of the absolute value of imaginary parts. It is obvious that trajectories overlap each other when $-0.5 \leq L_I \leq 0$ for the same conductivity with various tilting angles. This means that the effect from the tilting angle could be almost removed with only the overlap part of the trajectory taken into consideration for classifying the conductivity.

III. EXTRACTION OF GLOBAL FEATURES

To remove the effect from tilting angles, we first normalize the measured mutual inductance to the maximum of the absolute value of the imaginary parts. The mutual inductance trajectories on the complex plane after normalization are plotted in Fig. 5 where trajectories overlap each other when $-0.5 \leq L_I \leq 0$ for the same conductivity with various tilting angles. This means that the effect from the tilting angle could be almost removed with only the overlap part of the trajectory taken into consideration for classifying the conductivity. The next step is to extract the global features of the overlap parts of trajectories. By merging the overlap parts of trajectories of different samples with the same tilting angle into one figure, it is observed that different trajectory has a different curvature which is able to be found by the circle fitting method, as shown in Fig. 6. Every trajectory has a distinct fitting circle. The global features for one trajectory are the radius and the circle center of the fitting circle. In this article, it is enough to achieve the conductivity classification by only using the circle center. The method of circle fitting is given below

$$(x-a)^2 + (y-b)^2 = R^2 \tag{5}$$

where (a, b) is the circle center, R is the radius of the fitting circle. To obtain a, b and R, we transform the circle equation

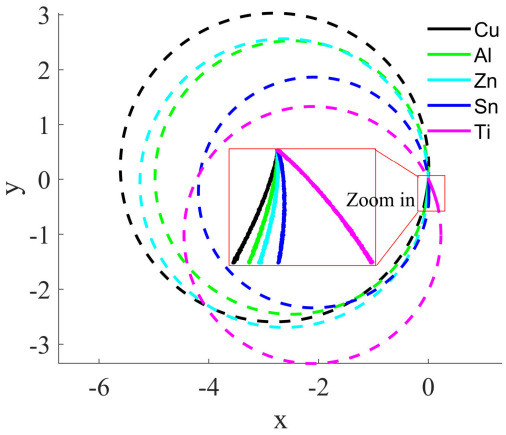

FIGURE 6. Fitting circles of different samples with the same tilting angle 8.5°. It is apparent that every trajectory has a distinct fitting circle. The global features for one trajectory contain the radius and the circle center of the fitting circle.

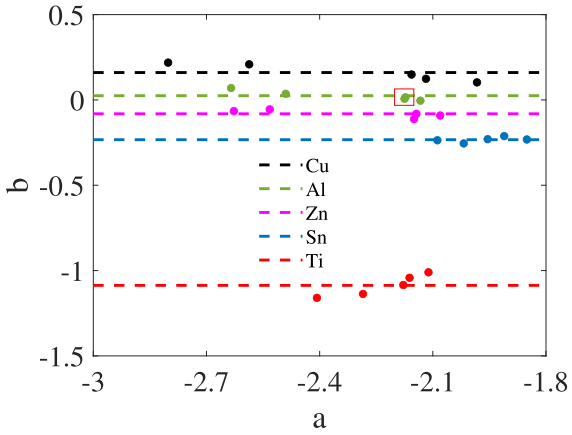

FIGURE 7. Distribution of fitting circle centers among which dots are all distributed near the dashed line of the same color (dots of the same color are the circle centers for the same sample with different tilting angles). The classification technique is based on finding the minimum distance between the fitting circle center of the input measurements and all the dashed lines. Dashed lines denote $b = \overline{b_i}$ (where $\overline{b_i}$ are arithmetic means of b_{ij}, the longitudinal coordinates of the fitting circle centers for the same conductivity with different tilting angles). Two dots in the red square overlap each other.

into the matrix form given by

$$[x_k^2 + y_k^2]_{n\times 1} = \begin{bmatrix}[x_k]_{n\times 1} & [y_k]_{n\times 1} & [e_k]_{n\times 1}\end{bmatrix} \times \begin{bmatrix} 2a \\ 2b \\ R^2 - a^2 - b^2 \end{bmatrix} \quad (6)$$

where n is the dimension of the data and $e_k = 1$. Since x_k and y_k are known, a, b and R is obtainable so long as we solve the matrix in MATLAB R2020a by

$$\begin{bmatrix} 2a \\ 2b \\ R^2 - a^2 - b^2 \end{bmatrix} = \begin{bmatrix}[x_k]_{n\times 1} & [y_k]_{n\times 1} & [e_k]_{n\times 1}\end{bmatrix} \backslash [x_k^2 + y_k^2]_{n\times 1} \quad (7)$$

IV. CONDUCTIVITY CLASSIFICATION TECHNIQUE

Although the conductivity classification has been realized by many methodologies of electromagnetic induction such as magnetic induction spectroscopy [24], eddy current measurement [16], and so forth, none of these researches has considered samples with tilting surfaces. Our previous research has first utilized photoelectric sensors to obtain the tilting angle and then resorted to eddy current sensors to find the conductivity after the phase compensation [8]. Even though the samples with tilting surfaces within 9.0° could be classified, more complexity and error are actually involved in the whole system by combining two types of sensors and using the method of linear fitting twice. The technique developed in this article extends the classifiable tilting angle range from 0 ∼ 9.0° to 0 ∼ 11.3° with higher classification accuracy by only using eddy current sensors. The principle of the circle fitting method has been introduced in Section III. After applying the circle fitting method to all the overlap parts of trajectories in Fig. 5, these fitting circle centers are plotted in Fig. 7. The black dots are all distributed near the black dashed line (which is designated the feature line for copper) and so are the other dots. It is also observed that the larger conductivity is, the higher the feature line is. This is explainable since the overlap part of the trajectory is rotating clockwise with conductivity increasing in Fig. 6, whose corresponding circle center would become lower. It is the feature lines $b = \overline{b_i}$ (where $\overline{b_i}$ are arithmetic means of b_{ij}, the longitudinal coordinates of the fitting circle centers for the same conductivity with different tilting angles) and corresponding deviations $\pm|\delta_i|$ that construct different ranges $[\overline{b_i}-|\delta_i|, \overline{b_i}+|\delta_i|]$. It is the fact that these ranges have no intersection with each other that provides the conductivity classification with enough fidelity, as shown in Table 2.

TABLE 2. Feature line (dashed lines in Fig. 7) and deviation (the maximum difference between longitudinal coordinates of the fitting circle centers of the same color in Fig. 7).

Features/Metal	Feature line	deviation
Copper	b=0.161	± 0.058
Aluminum	b=0.025	± 0.045
Zinc	b=-0.081	± 0.031
Tin	b=-0.233	± 0.022
Titanium	b=-1.087	± 0.077

The classification of conductivity is intuitive in that only two steps are needed. First find the distances between the input circle center (A, B) and different feature lines; then search for the minimum distance whose corresponding conductivity is the output. The mathematical expressions are

TABLE 3. Validation results where the input circle center is extracted by using the method of circle fitting on mutual inductance obtained experimentally, d_i denotes the distance between the input circle center and five feature lines, i is the location of the minimum distance and d is the minimum distance.

Test metal	Tilting angle	Input circle center	$\{d_i\}$	[i, d]
Copper	2.9°	(-2.157, 0.149)	$\{0.012, 0.124, 0.230, 0.382, 1.236\}$	[1, 0.012]
Aluminum	0°	(-2.133, -0.004)	$\{0.165, 0.029, 0.077, 0.229, 1.083\}$	[2, 0.029]
Zinc	8.5°	(-2.627, -0.065)	$\{0.226, 0.090, 0.016, 0.168, 1.022\}$	[3, 0.016]
Tin	11.3°	(-1.911, -0.212)	$\{0.373, 0.237, 0.131, 0.021, 0.875\}$	[4, 0.021]
Titanium	5.7°	(-2.162, -1.042)	$\{1.203, 1.067, 0.961, 0.809, 0.045\}$	[5, 0.045]

Note: i=1 for Cu; 2 for Al; 3 for Zn; 4 for Sn; 5 for Ti

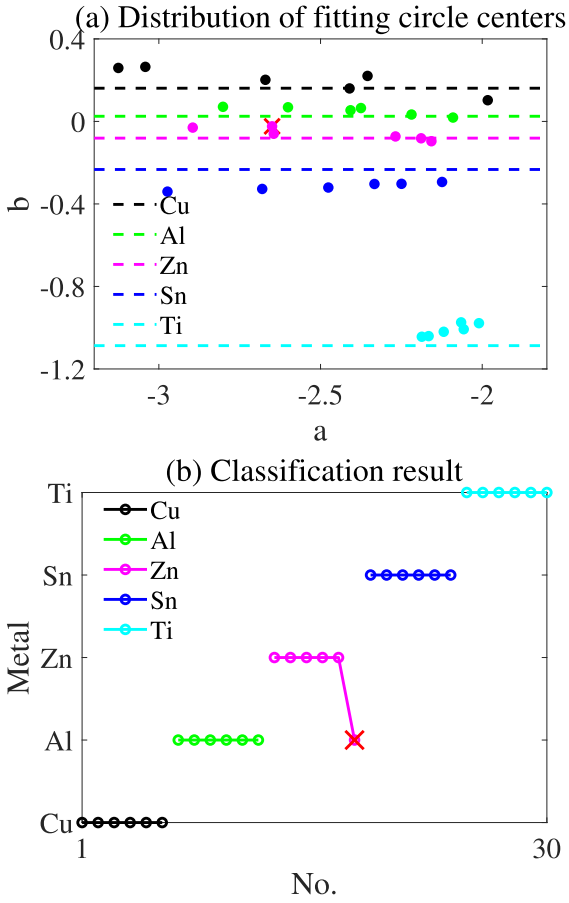

FIGURE 8. Test results are shown in two forms. (a) Distribution of fitting circle centers. (b) Classification result. The tilting angle is varying from 0° to 14.0°. The red cross denotes the wrong test where the sample of zinc is tilted with the angle 14.0°.

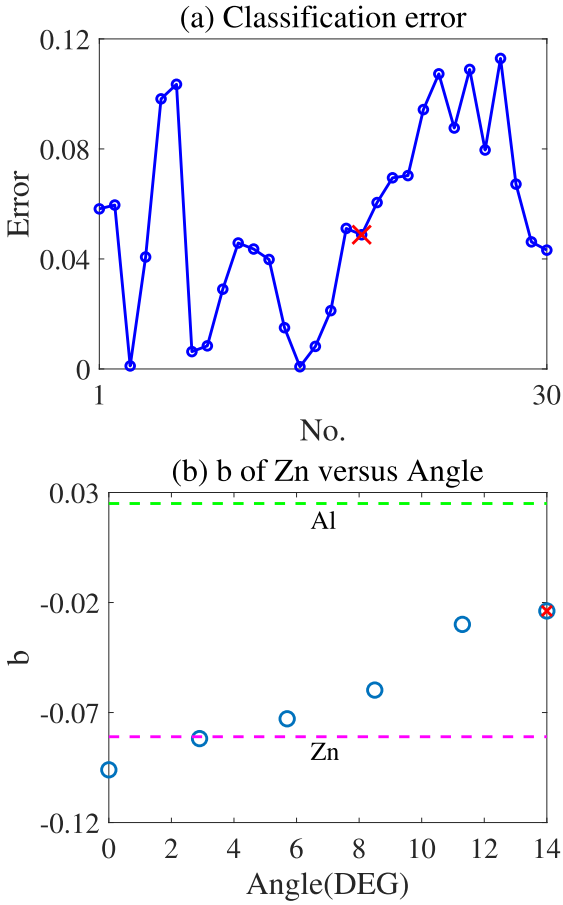

FIGURE 9. (a) Classification error (the minimum distance between the fitting circle center and five featuer lines). (b) Error analysis of Zn. The red cross denotes the wrong test. The b is the longitudinal coordinate of the circle center of the fitting circle.

given by

$$d_i = |B - \overline{b_i}| \tag{8}$$

where d_i is the distance and $y = \overline{b_i}$ is the feature line.

$$[i, d] = min\{d_i\} \tag{9}$$

where i is the label of metal and d is the minimum distance. The validation results using this classification technique are shown in Table 3 where all inputs could be accurately classified. To prove the advancement of this technique on classifying the conductivity with larger tilting angles, we conduct tests for 30 times with the tilting angle varying from 0° to 14.0°. The fitting circle centers are plotted in Fig. 8(a) with only one wrong test denoted by a red cross. As is shown in Fig. 8(b) when the tilting angle is smaller than 11.3°,

the samples are all successfully classified. To find out the effect on classification accuracy from further increasing the tilting angle, the test results of 14.0° are also obtained. The total classification rate is 96.7% within 14.0°. As is shown in Fig. 9(a), the No. 18 test is wrong, where the tilting angle for Zn is 14.0°. The reason is that the fitting circle center of zinc with the tilting angle of 14.0° is closer to the feature line of aluminum, which is obviously shown in Fig. 9(b). Thus, further increasing the tilting angle would decrease the classification accuracy.

V. CONCLUSION

This article manages to obtain the mutual inductance trajectory that is single-valued based on a different set-up from the one in [8]. The single-valued curve makes it possible to extract global features to represent different trajectories of different conductivity. To resolve the issue of classifying metallic scraps with tilting surfaces that may happen in the practical classification process, we propose the circle fitting method to extract global features that can remove the effect from tilting surfaces based on the fact that the same parts of mutual inductance trajectories for the same conductivity with different tilting angles overlap. One of the extracted global features-the fitting circle center-is used to classify the conductivity. These circle centers for the same conductivity but with different tilting angles actually scatter in the neighborhood of a feature line. After obtaining the functions of these feature lines, a two-step classification algorithm is formed on the basis of finding the minimum distance between the input circle center and five feature lines. The test results show that inputs are accurately classified within 11.3°. Theoretically, any other metallic samples, as long as it shows similar single-valued curves to those in Fig. 6, could be included in Fig. 7 with different feature lines. Furthermore, this classification technique may be applicable to not only the tilting angle but also other variables. It is reasonable to envision that the alloys that have the same conductivity are also possible to own fitting circle centers which are scattered near the feature line belonging to the corresponding conductivity. Thus, this classification technique has great potential to be applicable to a lot of situations. Since this classification system involves nothing but eddy current sensors, it is easy to be integrated with other functional eddy-current systems (such as systems for measuring coating thickness [15], measuring displacement [25], and so forth) to classify the conductivity simultaneously.

REFERENCES

[1] L. Svarovsky, "Introduction to solid-liquid separation," in *Solid-Liquid Separation*. Amsterdam, The Netherlands: Elsevier, 2001, pp. 1–29.

[2] A. Picón, O. Ghita, P. F. Whelan, and P. M. Iriondo, "Fuzzy spectral and spatial feature integration for classification of nonferrous materials in hyperspectral data," *IEEE Trans. Ind. Informat.*, vol. 5, no. 4, pp. 483–494, Nov. 2009.

[3] G. Candiani, N. Picone, L. Pompilio, M. Pepe, and M. Colledani, "Characterization of fine metal particles derived from shredded WEEE using a hyperspectral image system: Preliminary results," *Sensors*, vol. 17, no. 5, p. 1117, May 2017.

[4] R. Noll, V. Sturm, U. Aydin, D. Eilers, C. Gehlen, M. Höhne, A. Lamott, J. Makowe, and J. Vrenegor, "Laser-induced breakdown spectroscopy—From research to industry, new frontiers for process control," *Spectrochimica Acta B, At. Spectrosc.*, vol. 63, no. 10, pp. 1159–1166, 2008.

[5] S. P. Gundupalli, S. Hait, and A. Thakur, "A review on automated sorting of source-separated municipal solid waste for recycling," *Waste Manage.*, vol. 60, pp. 56–74, Feb. 2017.

[6] M. B. Mesina, T. P. R. de Jong, and W. L. Dalmijn, "Automatic sorting of scrap metals with a combined electromagnetic and dual energy X-ray transmission sensor," *Int. J. Mineral Process.*, vol. 82, no. 4, pp. 222–232, Jun. 2007.

[7] W. L. Dalmijn and T. P. R. De Jong, "The development of vehicle recycling in Europe: Sorting, shredding, and separation," *JOM*, vol. 59, no. 11, pp. 52–56, Nov. 2007.

[8] Y. Du, Z. Zhang, W. Yin, S. Zhu, Z. Chen, and H. Xu, "Conductivity classification of non-magnetic tilting metals by eddy current sensors," *Sensors*, vol. 20, no. 9, p. 2608, May 2020.

[9] A. Sophian, G. Y. Tian, D. Taylor, and J. Rudlin, "Design of a pulsed eddy current sensor for detection of defects in aircraft lap-joints," *Sens. Actuators A, Phys.*, vol. 101, nos. 1–2, pp. 92–98, Sep. 2002.

[10] M. Lu, H. Xu, W. Zhu, L. Yin, Q. Zhao, A. Peyton, and W. Yin, "Conductivity lift-off invariance and measurement of permeability for ferrite metallic plates," *NDT E Int.*, vol. 95, pp. 36–44, Apr. 2018.

[11] W. Yin and A. J. Peyton, "Thickness measurement of non-magnetic plates using multi-frequency eddy current sensors," *NDT E Int.*, vol. 40, no. 1, pp. 43–48, Jan. 2007.

[12] W. Yin, J. Tang, M. Lu, H. Xu, R. Huang, Q. Zhao, Z. Zhang, and A. Peyton, "An equivalent-effect phenomenon in eddy current non-destructive testing of thin structures," *IEEE Access*, vol. 7, pp. 70296–70307, 2019.

[13] Y. Yu, D. Zhang, C. Lai, and G. Tian, "Quantitative approach for thickness and conductivity measurement of monolayer coating by dual-frequency eddy current technique," *IEEE Trans. Instrum. Meas.*, vol. 66, no. 7, pp. 1874–1882, Jul. 2017.

[14] J. Xu, J. Wu, W. Xin, and Z. Ge, "Measuring ultrathin metallic coating properties using swept-frequency eddy-current technique," *IEEE Trans. Instrum. Meas.*, vol. 69, no. 8, pp. 5772–5781, Aug. 2020.

[15] H. Wang, W. Li, and Z. Feng, "Noncontact thickness measurement of metal films using eddy-current sensors immune to distance variation," *IEEE Trans. Instrum. Meas.*, vol. 64, no. 9, pp. 2557–2564, Sep. 2015.

[16] C. Wang, M. Fan, B. Cao, B. Ye, and W. Li, "Novel noncontact eddy current measurement of electrical conductivity," *IEEE Sensors J.*, vol. 18, no. 22, pp. 9352–9359, Nov. 2018.

[17] G. Y. Tian and A. Sophian, "Reduction of lift-off effects for pulsed eddy current NDT," *NDT E Int.*, vol. 38, no. 4, pp. 319–324, Jun. 2005.

[18] Y. Yu, Y. Yan, F. Wang, G. Tian, and D. Zhang, "An approach to reduce lift-off noise in pulsed eddy current nondestructive technology," *NDT E Int.*, vol. 63, pp. 1–6, Apr. 2014.

[19] H. Xu, J. R. Salas Avila, F. Wu, M. J. Roy, Y. Xie, F. Zhou, A. Peyton, and W. Yin, "Imaging x70 weld cross-section using electromagnetic testing," *NDT E Int.*, vol. 98, pp. 155–160, Sep. 2018.

[20] Z. Chen, J. R. Salas-Avlia, Y. Tao, W. Yin, Q. Zhao, and Z. Zhang, "A novel hybrid serial/parallel multi-frequency measurement method for impedance analysis in eddy current testing," *Rev. Sci. Instrum.*, vol. 91, no. 2, Feb. 2020, Art. no. 024703.

[21] C. V. Dodd and W. E. Deeds, "Analytical solutions to eddy-current probe-coil problems," *J. Appl. Phys.*, vol. 39, no. 6, pp. 2829–2838, May 1968.

[22] R. Huang, M. Lu, A. Peyton, and W. Yin, "Thickness measurement of metallic plates with finite planar dimension using eddy current method," *IEEE Trans. Instrum. Meas.*, early access, Apr. 13, 2020, doi: 10.1109/TIM.2020.2987413.

[23] W. Yin, R. Binns, S. J. Dickinson, C. Davis, and A. J. Peyton, "Analysis of the liftoff effect of phase spectra for eddy current sensors," *IEEE Trans. Instrum. Meas.*, vol. 56, no. 6, pp. 2775–2781, Dec. 2007.

[24] M. D. O'Toole, N. Karimian, and A. J. Peyton, "Classification of nonferrous metals using magnetic induction spectroscopy," *IEEE Trans. Ind. Informat.*, vol. 14, no. 8, pp. 3477–3485, Aug. 2018.

[25] Y. Yu, G. Tian, X. Li, and A. Simm, "An approach to ERO problem in displacement eddy current sensor," *Nondestruct. Test. Eval.*, vol. 28, no. 3, pp. 195–207, Sep. 2013.

YUE DU received the B.S. degree from the School of Physics, Liaoning University, Shenyang, China. She is currently pursuing the M.S. degree with the School of Instrument and Electronics, North University of China, Shanxi, China. Her research interests include non-destructive testing, conductivity classification, and EMT imaging.

ZHIJIE ZHANG (Member, IEEE) received the B.Sc. degree in automation instrumentation from Tianjin University, Tianjin, China, in 1986, and the Ph.D. degree in mechatronic engineering from the Beijing Institute of Technology, Beijing, China, in 1998. He is currently a Professor with the School of Instrument and Electronics, North University of China, Taiyuan, Shanxi, China.

WULIANG YIN (Senior Member, IEEE) received the B.Sc. and M.Sc. degrees in electronic measurement and instrumentation from Tianjin University, Tianjin, China, in 1992 and 1995, respectively, and the Ph.D. degree in automotive electronics from Tsinghua University, Beijing, China, in 1999. He was appointed as a Mettler Toledo (MT) Sponsored Lecturer with the Department of Electrical and Electronic Engineering, School of Engineering, The University of Manchester, Manchester, U.K., in 2012, where he was promoted to a Senior Lecturer, in 2016. He has authored one book and more than 230 articles. He was granted more than ten patents in the area of electromagnetic sensing and imaging. He was a recipient of the 2014 and 2015 Williams Award from the Institute of Materials, Minerals and Mining and the Science and Technology Award from the Chinese Ministry of Education, in 2000.

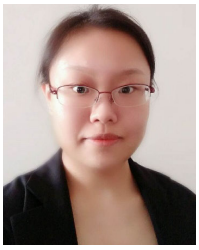

SHUANG ZHU received the B.Eng. degree in electronic science and technology from the Beijing University of Chemical Technology, Beijing, China, in 2017. She is currently pursuing the master's degree with the Department of Electrical and Electronic Engineering, The University of Manchester, Manchester, U.K. Her research interests include non-destructive testing, eddy current testing, and so on.

HANYANG XU received the B.Eng. and M.Sc. degrees in electrical and electronic engineering from The University of Manchester, in 2013 and 2014, respectively, where he is currently pursuing the Ph.D. degree in sensing and imaging. His current research interest includes non-destructive testing based on electromagnetic method.

ZIQI CHEN received the B.Sc. degree in eletronic and eletrical engineering from The University of Manchester, Manchester, U.K., in 2018, where she is currently pursuing the Ph.D. degree with the Department of Electrical and Electronic Engineering. Her current research interest includes developing hardware for electromagnetic sensing techniques, such as electromagnetic tomography (EMT) and multi-frequency electromagnetic testing.